Journal of Low Temperature Physics, Vol. 104, Nos. 5/6, 1996

Quantum Evaporation from the Free Surface of Superfluid ^{4}He

F. Dalfovo,[a] A. Fracchetti,[a] A. Lastri,[a, b] L. Pitaevskii,[c, d] and S. Stringari[a]

[a]*Dipartimento di Fisica, Università di Trento, and Istituto Nazionale di Fisica della Materia, I-38050 Povo, Italy*
[b]*Institut für Theoretische Physik, Universität zu Köln, D-50937 Köln, Germany*
[c]*Department of Physics, TECHNION, Haifa 32000, Israel*
[d]*Kapitza Institute for Physical Problems, ul. Kosygina 2, 117334 Moscow*

(Received March 14, 1996; revised May 10, 1996)

The scattering of atoms and rotons at the free surface of superfluid ^{4}He is studied in the framework of linearised time dependent mean field theory. The phenomenological Orsay–Trento density functional is used to solve numerically the equations of motion for the elementary excitations in presence of a free surface and to calculate the flux of rotons and atoms in the reflection, condensation, and evaporation processes. The probability associated with each process is evaluated as a function of energy, for incident angles such that only rotons and atoms are involved in the scattering (phonon forbidden region). The evaporation probability for R^+ rotons (positive group velocity) is predicted to increase quite rapidly from zero, near the roton minimum, to 1 as the energy increases. Conversely the evaporation from R^- rotons (negative group velocity) remains smaller than 0.25 for all energies. Close to the energy of the roton minimum, Δ, the mode-change process $R^+ \leftrightarrow R^-$ is the dominant one. The consistency of the results with general properties of the scattering matrix, such as unitarity and time reversal, is explicitly discussed. The condensation of atoms into bulk excitations is also investigated. The condensation probability is almost 1 at high energy in agreement with experiments, but it lowers significantly when the energy approaches the roton minimum in the phonon forbidden region.

1. INTRODUCTION

One of the unique features of superfluid helium at low temperature is that elementary excitations like rotons and high energy phonons have a very long mean free path, long enough to propagate ballistically in the liquid on macroscopic distances. Furthermore their energy is comparable with the energy required to eject atoms from liquid to vacuum. Thus rotons

0022-2291/96/0900-0367$09.50/0

and phonons impinging on the free surface of the liquid can evaporate atoms by one-to-one quantum processes. One can also produce collimated beams of elementary excitations and collect the evaporated atoms above the surface in order to extract information on the properties of the superfluid. Similarly one can investigate the opposite process of atoms which condense in the liquid by producing elementary excitations. Several experiments have been carried out in the last decades[1–10] to explore the phenomenon of quantum evaporation and condensation (see also Ref. 11 for a recent review). From the theoretical viewpoint[12–19] these processes are very appealing, being clean examples of scattering of excitations in a highly correlated many-body quantum system. A good theory of quantum evaporation and condensation is however a difficult task and a clear understanding of the fundamental mechanisms underlying these phenomena has still to come, even though relevant steps in this direction have been accomplished in the last years.

In this paper we present a time dependent mean field theory, based on the density functional formalism, which allows one to calculate the scattering matrix elements associated with the scattering of rotons, phonons and atoms at the free surface. Preliminary results of this theory have been recently published in Ref. 19. Here we discuss the theory in more detail and we present results in a wider range of energy and wave vectors.

A discussion about quantum evaporation and condensation requires first a detailed knowledge of the spectrum of elementary excitations of superfluid ^{4}He. A schematic picture is given in Fig. 1. The liquid-vacuum interface is supposed to be in the xy-plane. The system is translational invariant in those directions, so that the parallel wave vector q_x is a conserved quantity (we choose $q_y = 0$ without any loss of generality). The minimum energy needed to produce free atom states outside the liquid at zero temperature is the chemical potential $|\mu| = 7.15$ K. The threshold for evaporation for given values of q_x is then $|\mu| + \hbar^2 q_x^2/2m$ (dashed line). Phonons, rotons and atoms can propagate at different angles with respect to the surface, that is with different q_z for a given q_x. The dispersion law for phonons and rotons propagating in the bulk liquid and in the direction parallel to the surface ($q_z = 0$) is plotted as a function of q_x. Excitations having $q_z \neq 0$ fill different regions of the spectrum in Fig. 1 with a continuum of states. For instance each point in region V corresponds to a roton R^+ (positive group velocity) propagating with $q = \sqrt{q_x^2 + q_z^2}$ such that $\hbar\omega(q)$ is the R^+ roton dispersion. Since $q_x \leqslant q$, roton states with $q_z \neq 0$ fill the region at the left of the roton branch plotted in the figure. Similarly in region IV also R^- rotons (negative group velocity) can propagate; each point in that region can be a combination of R^+ and R^- rotons

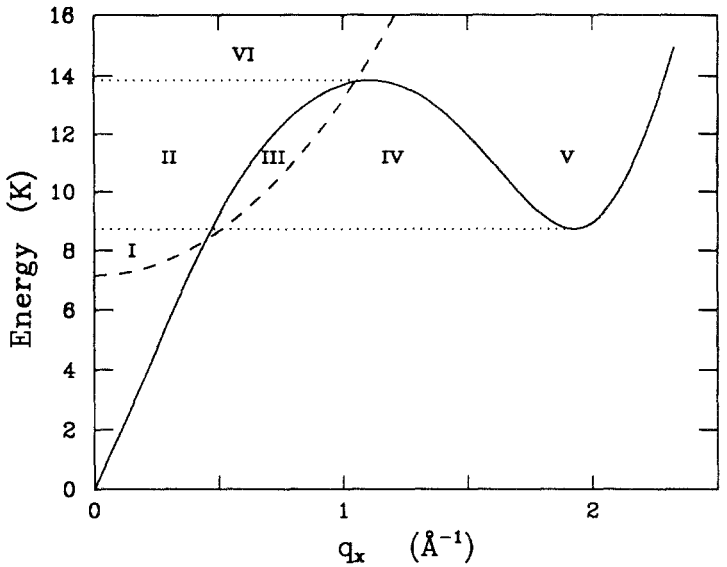

Fig. 1. Schematic picture for the spectrum of elementary excitations in presence of a free surface. Solid line: phonon-roton dispersion for excitations propagating in the direction parallel to the surface ($q_z = 0$). Dashed line: threshold for atom evaporation. Excitations propagating at different angles ($q_z \neq 0$) fill regions I–VI, as explained in the text.

propagating at different angles. Above the threshold for evaporation, in region III, atom states outside the liquid are possible too. Similarly in region II one has phonons, rotons as well as atoms; in region I, below the energy of the roton minimum, Δ, there are only phonons and atoms; finally in region VI, above the maxon energy, there are rotons and atoms. The free surface acts as a scattering region for all these excitations.

In Refs. 17, 18 the effect of the surface on the propagation of the elementary excitations has been studied within a local density approximation. The dispersion law of the excitations was assumed to be the same as for a uniform liquid of density equal to the local density. Maris[17] used a simple interpolation between the phonon-roton dispersion law in bulk liquid and the dispersion law of the free atoms. He studied the behavior of classical trajectories for quasiparticles along the z-direction assuming the conservation of energy and parallel momentum. From that analysis one finds some interesting constraints on the structure of the classical trajectories crossing the free surface. For instance only phonons and rotons above the maxon energy (about 14 K) are found to evaporate atoms. Vice-versa, the theory predicts no evaporation from rotons with energy smaller

than the maxon energy, because of the occurrence of a barrier at the interface. The experimental evidence[11] for quantum evaporation induced by rotons even below the maxon energy is consequently an important indication of the crucial role played by quantum effects. Quantum effects were partially included in the calculations of Ref. 18 by means of perturbation theory based on WKB states; the density profile in that case was approximated by a suitable analytic function and the dispersion law for the excited states, in local density approximation, was calculated using Beliaev's theory with an effective interaction.

For an accurate treatment of quantum effects one has to go beyond the local density approximation and the semiclassical treatment. To accomplish the task we proceed in two distinct steps:

- We first evaluate the ground state and the excited states of the inhomogeneous system within a self-consistent theory sufficiently accurate to reproduce the main features of the spectrum in Fig. 1, including the structure and the excitations of the free surface.
- We identify the current carried by the elementary excitations and use the numerical solutions of the equations of motion to calculate the asymptotic flux of excitations associated with a given scattering process. While this identification is trivial in the description of free atoms in vacuum, it becomes less obvious in the liquid where manybody effects, present in this highly correlated system, must be properly included. Taking the ratios of incoming and outgoing fluxes one finally gets the evaporation and condensation probabilities, which are the final goal of the theory.

For the first step we use a time dependent mean field theory based on the least action principle applied to an energy functional $\int d\mathbf{r}\mathscr{H}[\Psi^*, \Psi]$. For the form of the functional we follow the recent proposal of Ref. 20. We consider linear variation of Ψ, in the form $(\Psi_0 + \delta\Psi)$, and expand $\delta\Psi$ in plane waves along the parallel direction. We restrict ourselves to variations of the energy linear in $\delta\Psi$. For this reason the theory describes only one-to-one processes (evaporation of one atom by one roton, creation of one roton by condensing one atom, etc.) and not processes involving more than two excitations (for example multi-phonon or multi-ripplon production in the atom condensation process). It is worth mentioning that some experiments by Wyatt and co-workers[5, 6, 11] support the idea that the evaporation of atoms from bulk excitations is essentially a one-to-one process, so that the use of a linear theory seems justified in this case. Conversely measurements of atom condensation[3, 9] point out an important role played by non linear effects associated with the creation of ripplons. This

asymmetry between evaporation and condensation is still basically unexplained. Quantitative predictions for the scattering rates in linear theory are essential in order to better understand the origin of this and other discrepancies.

As concerns the second step we derive the definition of flux (or current density) associated with the propagation of the elementary excitations, in terms of the linearised solutions of the equations of motion. We show that such a current density obeys the proper equation of continuity. We will devote detailed discussions about the meaning of the flux of excitations and about the properties of the scattering matrix elements, which are calculated starting from the knowledge of the fluxes involved in the scattering process.

The theory can be applied to all the relevant regions of the spectrum in Fig. 1. In the present work we present results for processes involving rotons and atoms in the region III. We chose this region for two basic reasons: first, phonons are not allowed there and thus the analysis is simpler; second, the arguments based on classical trajectories predict no evaporation in this region and this means that quantum effects should play a crucial role in the evaporation process. The analysis of the remaining parts of the spectrum will be the object of a future work.

The paper is organised as follows: in Sec. 2 we present the theoretical formalism of the density functional and the equations of motion. In Sec. 3 we introduce the concept of current of excitations. In Sec. 4 we discuss general properties of the scattering matrix. In Sec. 5 we present the results for the probabilities of evaporation and condensation. Finally we will give a brief summary of the main results and discuss some future perspectives.

2. TIME DEPENDENT DENSITY FUNCTIONAL THEORY

The formalism used in the present work was already introduced in Ref. 20. In that paper detailed discussions were devoted to the motivations of the theory and to the choice of the density functional. Results for static and dynamic properties of superfluid ^{4}He in different geometries were presented. In Refs. 21 and 22, the dynamics of the free surface and of droplets, respectively, were studied in detail within the same scheme. As a consequence we refer to the above-mentioned papers for details and we recall here simply the main points.

The starting assumption is that the energy can be written as a functional of the form

$$E = \int d\mathbf{r}\, \mathscr{H}[\Psi, \Psi^*] \tag{1}$$

where the complex function Ψ is written as

$$\Psi(\mathbf{r}, t) = \Phi(\mathbf{r}, t) \exp\left(\frac{i}{\hbar} S(\mathbf{r}, t)\right). \tag{2}$$

The real function Φ is related to the diagonal one-body density by $\rho = \Phi^2$. The phase S fixes the velocity of the fluid through the relation $\mathbf{v} = (1/m)\nabla S$, where m is the mass of the ^{4}He atoms. In the calculation of the ground state only states with zero velocity must be considered, so that the energy is a functional only of the particle density $\rho(\mathbf{r})$. A natural representation is given by

$$E = \int d\mathbf{r}\, \mathcal{H}_0[\rho] = E_c[\rho] + \int d\mathbf{r}\, \frac{\hbar^2}{2m} (\nabla \sqrt{\rho})^2, \tag{3}$$

where the second term on the r.h.s. is a quantum pressure, corresponding to the kinetic energy of a Bose gas of non uniform density. The quantity $E_c[\rho]$ is a *correlation energy*; it incorporates the effects of dynamic correlations induced by the interaction. Ground state configurations are obtained by minimising the energy of the system with respect to the density. This leads to the Hartree-type equation

$$(H_0 - \mu)\sqrt{\rho(\mathbf{r})} = 0, \tag{4}$$

where

$$H_0 = -\frac{\hbar^2}{2m}\nabla^2 + U[\rho, \mathbf{r}] \tag{5}$$

is an effective Hamiltonian. The quantity $U[\rho, \mathbf{r}] \equiv \delta E_c / \delta \rho(\mathbf{r})$ acts as a mean field, while the chemical potential μ is introduced in order to ensure the proper normalisation of the density to a fixed number of particles. The dynamics of the system can be studied by using the least action principle:

$$\delta \int_{t_1}^{t_2} dt \int d\mathbf{r} \left[\mathcal{H}[\Psi^*, \Psi] - \mu \Psi^* \Psi - \Psi^* i\hbar \frac{\partial \Psi}{\partial t} \right] = 0. \tag{6}$$

By making variations with respect to Ψ or Ψ^* one derives the equations of motion for the excited states, in the form of Schrödinger-like equations. The equation for Ψ is

$$(H - \mu)\Psi = i\hbar \frac{\partial}{\partial t} \Psi, \tag{7}$$

where $H = \delta E/\delta \Psi^*$ is an effective Hamiltonian. We linearise the equation by writing

$$\Psi(\mathbf{r}, t) = \Psi_0(\mathbf{r}) + \delta\Psi(\mathbf{r}, t) \tag{8}$$

where $\Psi_0(\mathbf{r})$ corresponds to the ground state. The change of wave function $\delta\Psi$ can be written in the form

$$\delta\Psi(\mathbf{r}, t) = f(\mathbf{r})\, e^{-i\omega t} + g^*(\mathbf{r})\, e^{i\omega t}, \tag{9}$$

where the functions $f(\mathbf{r})$ and $g(\mathbf{r})$ are fixed, together with the frequency ω, by the solution of the equations of motion (7). The Hamiltonian H then takes the form

$$H = H_0 + \delta H \tag{10}$$

and the equation of motion becomes

$$(H_0 - \mu)\, \delta\Psi + \delta H\, \Psi_0 = i\hbar \frac{\partial}{\partial t} \delta\Psi. \tag{11}$$

The term δH is linear in $\delta\Psi$ and accounts for changes in the Hamiltonian induced by the collective motion of the system. Since H depends explicitly on the wave function Ψ, Equation (7) has to be solved using a self-consistent procedure.

The above scheme corresponds to a time dependent density functional (TDDF) theory. A discussions about equivalent formulations of the same approach (hydrodynamic-like equations, Green's functions), as well as about the connection with other many body approaches, is given in Refs. 20–22. Equations of the same type are obtained using Correlated Basis Functions in the context of Hypernetted Chain approximation.[23] Here we stress that the theory corresponds to a quantum mechanical treatment of the dynamics and consequently accounts for the interference and tunneling phenomena which are expected to play a crucial role in the evaporation process. Of course, due to linearisation, they do not include inelastic processes associated with multi-phonons or multi-ripplons. As already said in the Introduction, these effects lie beyond the present theory.

To proceed further one has to specify both the explicit form of the energy functional (1) and the geometry of the system under investigation. The energy functional is the one introduced in Ref. 20. It consists of two parts, a functional of the particle density only and a functional of both the particle density and the current density. It corresponds to a generalisation of a previous finite-range functional introduced by Dupont–Roc *et al.*[24] Its

explicit form is given in Appendix A. The functional is phenomenological, i.e., it contains parameters which are fixed to reproduce known properties of the bulk liquid. In particular the equation of state and the static response function in bulk liquid are reproduced by construction. The new functional, with respect to the one of Ref. 24, contains a current-current effective interaction, which accounts for backflow-like correlations and allows one to reproduce the experimental phonon-roton spectrum in the uniform liquid. The latter is a crucial requirement for a theory whose goal is the prediction of evaporation and condensation probabilities, since these quantities depend dramatically on the form of the excitation spectrum.

As concerns the geometry, we assume translational invariance in the $x-y$ plane. The density profile of the liquid in the ground state is a function of the orthogonal co-ordinate z. The profile of the free surface obtained with the present density functional theory is about 6 Å thick and compares well with the one coming from ab initio calculations as well as with the experimental data of Ref. 25 (see Ref. 22 for a discussion). The excited states are described by fluctuations of the particle density and velocity associated with the solutions (9) of the equations of motion. In the planar geometry the same solutions can be written in the form[26]

$$\delta\Psi(\mathbf{r}, t) = f(z)\, e^{i(q_x x - \omega t)} + g(z)\, e^{-i(q_x x - \omega t)}. \tag{12}$$

With a proper choice for the boundary conditions the functions $f(z)$ and $g(z)$ can be chosen real. Once the equations of motion are written explicitly for the unknowns $f(z)$ and $g(z)$, they assume the typical form of the equations of the random phase approximation (RPA) for bosons. In particular they account for both particle-hole $[f(z)]$ and hole-particle $[g(z)]$ transitions which are coupled by the equations of motion (6). This coupling is of crucial importance in order to treat the correlation effects associated with the propagation of elementary excitations in an interacting system. The equations of motion have also a structure formally identical to the one of the Bogoliubov equations for the dilute Bose gas[27] and to the one of the Beliaev equations for Bose superfluids.[18, 28] With respect to those theories the present approach makes use of a finite ranged and momentum dependent effective interaction. The same theory gives a reliable description of surface modes (ripplons) both at small and high momenta.[21] In the vacuum the equations of motion coincide with the Schrödinger equation for the free atom wave function $f(z)$, while $g(z)$ vanishes.

The equations for $f(z)$ and $g(z)$ are solved numerically in a finite box. We work in a slab geometry, that is, with the liquid confined within two parallel surfaces, the slab being centered in the box. The box size is of the order of $100 \div 150$ Å and the slab thickness is typically $50 \div 100$ Å to

simulate sufficiently well the semi-infinite medium. The space along z is represented by a mesh of points, with step $0.1 \div 0.15$ Å. The Hartree equation (4) for the ground state is solved by diffusing a trial wave function in imaginary time. After several iterations the procedure converges to the density profile which minimise the energy functional. The minimisation takes $2 \div 5$ hours of CPU-time on a workstation, depending on the accuracy required. The same calculation provides the self-consistent mean field entering the static Hamiltonian (5). Then we expand the linearised time dependent wave function $\delta\Psi$ on the basis of eigenstates of H_0. By this way the equations of motion for f and g become a matrix equation for the coefficients of the expansion. We take a basis of 100 states or more to cover all the relevant part of the spectrum, so that the matrix to diagonalise is at least of dimension 100×100. The solution of the equations of motion for a given value of parallel wave vector q_x takes about two hours of CPU-time on a workstation. The output is a set of discrete eigenenergies and the corresponding functions $f(z)$ and $g(z)$. By solving for different values of q_x one can span the whole spectrum. An example is shown in Fig. 2, where we plot the energies of the excitations of a slab 80 Å thick in a box of 150 Å. One recognises clearly the main features already reported in Fig. 1, namely

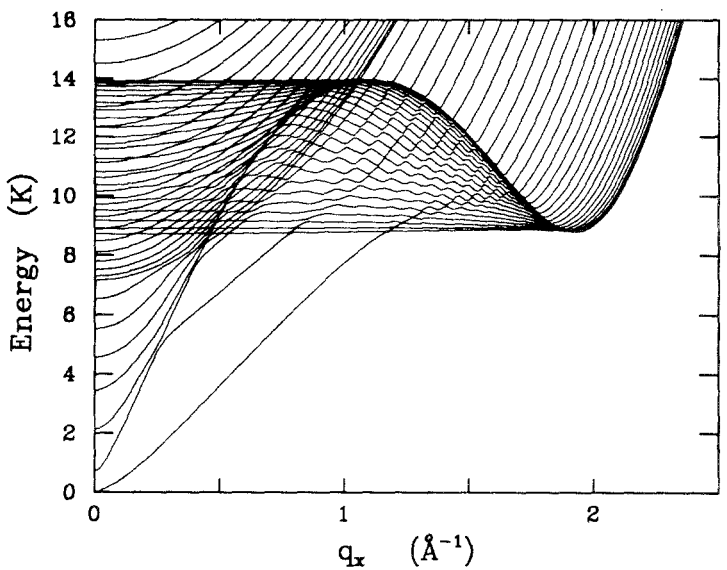

Fig. 2. Spectrum of elementary excitations for a slab 80 Å thick in a box 150 Å wide, as obtained solving numerically the TDDF equations. Two surface modes (ripplons) are also visible below the phonon-roton dispersion. For simplicity, only states symmetric with respect to the center of the slab are shown.

the phonon-roton dispersion and threshold for free atom states. The spacing in energy depends on the thickness of the slab and of the free space between the slab surface and the confining box. In the limit of infinite slab thickness the excitations in the liquid will reduce to a continuum of states, as already discussed for Fig. 1. In Fig. 2 one also notices lower branches below the roton energy Δ and the phonon dispersion. They correspond to surface modes and a discussion about them has been already reported in

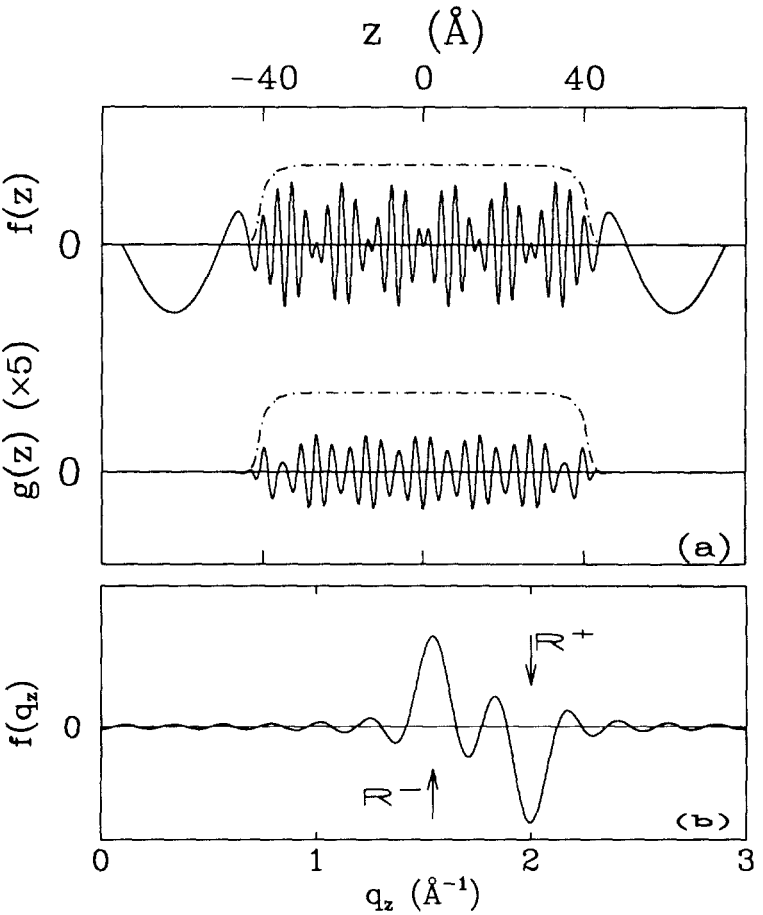

Fig. 3. Example of functions $f(z)$, in arbitrary units, and $g(z)$, in the same units but multiplied by 5, for a state at energy 10.2 K and parallel wave vector $q_x = 0.7$ Å^{-1} in the same slab as in Fig. 2. The density profile of the slab is shown as a dot-dashed line. In part *b*, the Fourier transform of $f(z)$ is shown; it corresponds to the convolution of two delta functions, at the R^+ and R^- roton wave vectors, with the transform of the step function used to restrict the Fourier analysis within the slab. The function $g(q_z)$, not shown, has a similar structure, but much smaller amplitude.

Ref. 21. The function f and g, at given q_x and ω, will take contributions from the elementary modes propagating inside and outside the liquid at different angles with respect to the surface. The contribution of each elementary mode (phonon, R^+ and R^- roton, atom, surface mode) is characterised by the appropriate dispersion law and can be identified by looking at the form of $f(z)$ and $g(z)$ and their Fourier transforms. An example is given in Fig. 3, where we show the form of $f(z)$ and $g(z)$ for one of the states of the spectrum in Fig. 2. The amplitude and the wave vector associated with the free atom are easily extracted from the form of $f(z)$ close to the boundary. The amplitudes and wave vectors of rotons can be calculated by looking at the Fourier transforms of $f(z)$ and $g(z)$ in the liquid. In the lower part of Fig. 3 we show the Fourier transform of $f(z)$. In the limit of infinite slab thickness, the function $f(q_z)$ would reduce to the sum of two δ-functions of the form $f_\pm \delta(q_z - q_{z\pm})$, corresponding to $R^\pm$ rotons. Since the Fourier analysis is restricted to a finite box within the slab, $f(q_z)$ is actually the convolution of those δ-functions with the transform of a step function; this convolution produces the oscillations visible in the figure. The amplitudes $f_\pm$ and the wave vectors $q_{z\pm}$ are extracted with great accuracy by fitting $f(q_z)$. In the case of Fig. 3b the best fit is indistinguishable from $f(q_z)$.

All these numerical results are used as input in the calculation of the flux of excitations in the scattering processes at the surface, as explained in the following section.

3. FLUX OF ELEMENTARY EXCITATIONS

In the standard theory of scattering the probability associated with a given output channel is written as the ratio between the outgoing flux in that channel and the incoming flux. In the case of quantum evaporation the free surface acts as scattering region and one has to consider the flux of elementary excitations, i.e., rotons, phonons and atoms. The solutions of the equations of motion provide the fluctuations of the density and current of helium atoms expressed by means of functions $f(z)$ and $g(z)$ entering $\delta\Psi$. These functions are different inside and outside the liquid and the boundary produces the appropriate matching between the excitations of the bulk liquid and the free atoms states in vacuum. Now one has to relate the asymptotic form of these functions with the flux of incoming and outgoing excitations in a given scattering process. We proceed in two steps. First we introduce the concept of current of elementary excitations within the formalism of linearised time dependent mean field theory. Then we represent the scattering processes by taking linear combinations of stationary solutions of the TDDF equations.

Far away from the surface and for a given energy $\hbar\omega$ the function $\delta\Psi$ is the sum of plane waves of the form

$$\delta\Psi(\mathbf{r}) = \sum_j [f_j(\mathbf{r})\, e^{-i\omega t} + g_j^*(\mathbf{r})\, e^{i\omega t}] = \sum_j [f_j e^{i(\mathbf{q}\cdot\mathbf{r}-\omega t)} + g_j e^{-i(\mathbf{q}\cdot\mathbf{r}-\omega t)}] \quad (13)$$

where the index $j = a, +, -$ refers to the type of excitations (atoms, R^+ and R^- respectively) which contributes to $\delta\Psi$. Each type of excitation obeys its own dispersion law $\omega(\mathbf{q})$ and contributes to $\delta\Psi$ with amplitudes f_j and g_j.

Well outside the liquid $\delta\Psi$ describes free atoms. The hole-particle part g_a vanishes, while the atom density is given by $\rho_a = f_a^2$. The density of current is given by

$$\mathbf{j}_a = \frac{\hbar\mathbf{q}}{m} f_a^2 = \mathbf{v}_a f_a^2, \quad (14)$$

where $\mathbf{v}$ is the group velocity which, for the free atoms, coincides with $\hbar\mathbf{q}/m$. These are the usual definitions of density and current density for free particles.

Inside the liquid the same definitions can be generalised to describe the elementary modes of the correlated system. The RPA (or, equivalently, Bogoliubov) formalism provides a natural generalization for the density of elementary excitations which, in term of the components f and g of the time dependent solution (9), is given by

$$\rho_j^{ex} \equiv |f_j(\mathbf{r})|^2 - |g_j(\mathbf{r})|^2 = f_j^2 - g_j^2. \quad (15)$$

This expression is consistent with the well known ortho-normalisation property of the RPA solutions:

$$\int d\mathbf{r}\, [f_i^*(\mathbf{r})\, f_j(\mathbf{r}) - g_i^*(\mathbf{r})\, g_j(\mathbf{r})] = \delta_{ij}. \quad (16)$$

The total density of elementary excitations, $\rho^{ex} = \sum_j \rho_j^{ex}$, satisfies the equation of continuity:

$$\frac{\partial \rho^{ex}}{\partial t} + \nabla \cdot \mathbf{j}^{ex} = 0. \quad (17)$$

The quantity $\mathbf{j}^{ex} = \sum_j \mathbf{j}_j^{ex}$ is identified with the current density of excitations, for which one expects the result

$$\mathbf{j}_j^{ex} = \mathbf{v}_j \rho_j^{ex} \equiv \mathbf{v}_j (f_j^2 - g_j^2) \quad (18)$$

where $\mathbf{v}_j = \nabla_{\mathbf{q}} \omega(q)$ is the group velocity of the jth elementary excitation. The group velocity should not be confused with the quantity $\hbar\mathbf{q}/m$ (which is the correct expression only for free atoms) and actually becomes opposite to $\mathbf{q}$ in the R^- range of wave vectors. In Appendix B we show that the form (18) for the current density is fully consistent with the equations for ρ_j^{ex} derived starting from the solutions of the TDDF equations. We note also that, when ρ^{ex} and $\mathbf{j}^{ex}$ are calculated by using the stationary solutions of the equations of motion, the time derivative vanishes and the equation of continuity implies simply that the z-component of the current of elementary excitations is equal inside and outside the liquid. This result is also connected with the unitarity of the scattering matrix, as we will discuss in the next section.

Equations (15, 17, 18) emphasise a remarkable feature of the TDDF solutions. In a dilute system they reduce to the usual expressions holding for free particles, while in the interacting liquid they include the correlations associated with the propagation of the collective modes. For instance in the long wavelength phonon regime ($q \to 0$) the group velocity coincides with the sound velocity and $g \simeq f$.

From the knowledge of the current of elementary excitations associated with each asymptotic solution one can calculate the flux of incoming and outgoing excitations in a scattering process. Actually the output of our TDDF equations, as discussed in Sec. II, are stationary solutions, namely real functions $f(z)$ and $g(z)$ which vanish at the border of the computational box. These functions can be viewed as a combination of R^+ and R^- rotons in the liquid and atoms outside, travelling to and from the surface as shown schematically in the upper part of Fig. 4. Using Eq. (18) one can calculate the current associated with each component. In order to select a single scattering process one can combine two or more stationary solutions at the same energy and parallel wave vector.[29] If $f^{(1)}(z)$, $f^{(2)}(z)$ and $f^{(3)}(z)$ are three solutions of the linearised TDDF equation at the same energy and parallel wave vector, then the combination

$$f(z) = f^{(1)}(z) + a_2 f^{(2)}(z) + a_3 f^{(3)}(z) \tag{19}$$

is also a solution (the same holds for $g(z)$). One can choose the coefficients of the combination in such a way that part of the incoming flux vanishes. For instance, if we want to represent one R^+ roton impinging onto the surface and reflecting as R^+ or R^-, or evaporating an atom, we have to combine the TDDF solutions in order to make the incoming fluxes of atoms and R^- rotons vanish. This provides two equations for the complex coefficients a_2 and a_3 in terms of the amplitudes $f^{(\alpha)}$ and $g^{(\alpha)}$ (the third coefficient a_1 fixes the normalization of the wave function and its value is

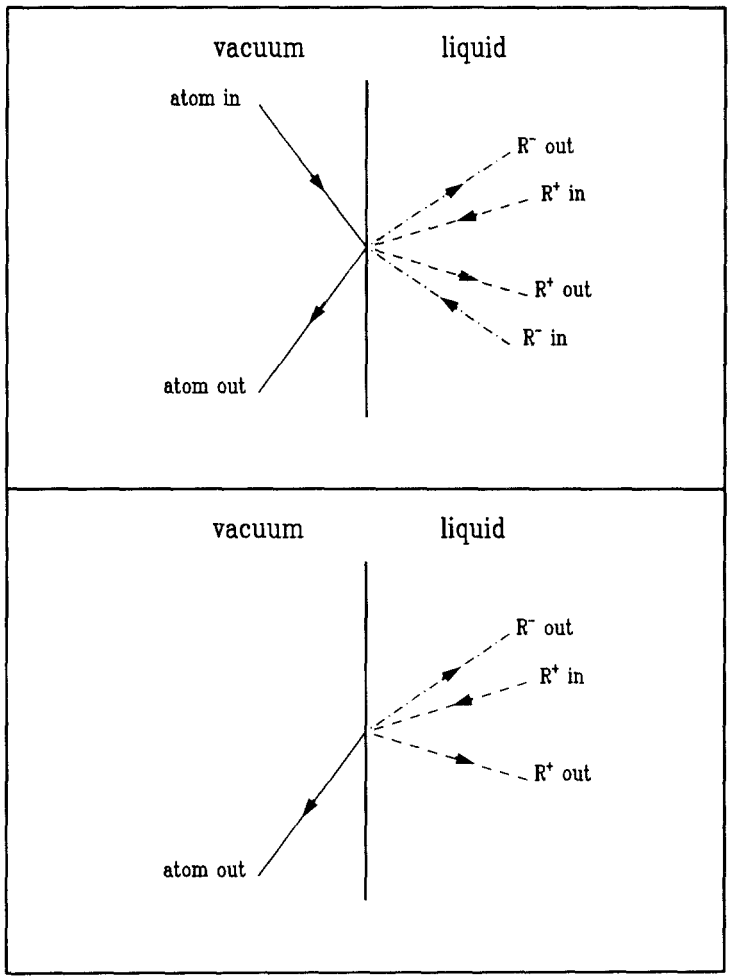

Fig. 4. Schematic picture for scattering processes at the free surface. In the lower part a particular process is selected: an incoming R^+ roton can produce atom evaporation, normal reflection or mode-change reflection.

not relevant when one calculates the ratio of fluxes). Once the coefficients are calculated, one is left with a solution which represents a flux (current density projected along z) of incoming R^+ rotons and a flux of evaporated atoms and reflected R^+ and R^- rotons, as in the lower part of Fig. 4. By definition, the evaporation probability is given by

$$P_{+a} = \frac{\text{flux of evaporated atoms}}{\text{flux of incoming } R^+} \tag{20}$$

the normal reflection probability is

$$P_{++} = \frac{\text{flux of reflected } R^+}{\text{flux of incoming } R^+} \tag{21}$$

and the mode-change reflection is

$$P_{+-} = \frac{\text{flux of reflected } R^-}{\text{flux of incoming } R^+}. \tag{22}$$

The explicit formulae for this scattering process, including the geometry of the slab and the box, are given in Appendix C. By combining the stationary solutions with different coefficients one can select the process in which the incident excitation is a R^- roton. In this case the ratios of the outgoing fluxes and the incoming R^- flux provide the probabilities P_{-a} (evaporation), P_{--} (normal reflection) and P_{-+} (mode-change reflection). Similarly, by selecting the process with an incident atom one gets the probabilities P_{aa} (reflection), P_{a+} (condensation in R^+) and P_{a-} (condensation in R^-). In region III of the spectrum in Fig. 1 these are the only one-to-one processes available. Generalisation to the other regions of the spectrum is straightforward.

The method we have used in Ref. 19 to derive the evaporation and reflection probabilities is simpler but less general. It corresponds to the case when one of the state in the linear combination has vanishing amplitude outside the liquid, due to destructive interference. The existence of such *resonant states* simplifies the calculation of the probabilities P_{ij}. However, the more general method used in the present work is not restricted to special states and provides results on a wider range of energy. Furthermore it can be easily extended to describe more scattering channels.

4. THE SCATTERING MATRIX

The scattering matrix S characterises a scattering process through the definition $\Psi_{out} = S\Psi_{in}$. The unitarity and the time reversal symmetry ($t \to -t$) of S imply

$$S^\dagger = S^{-1} \tag{23}$$

and

$$S^* = S^{-1} \tag{24}$$

respectively. Combining these two conditions one finds that the scattering matrix elements must satisfy the general property

$$S_{ij} = S_{ji}. \tag{25}$$

The scattering matrix elements are related to the probabilities P_{ij} by

$$P_{ij} = |S_{ij}|^2. \tag{26}$$

Equation (25) then implies that the evaporation, reflection and condensation rates, introduced in the previous section, reduce to six quantities to be calculated: P_{+a}, P_{-a}, P_{++}, P_{--}, P_{+-} and P_{aa}. Furthermore the unitarity condition takes also the form $S^*S = 1$, or

$$|S_{+a}|^2 + |S_{++}|^2 + |S_{+-}|^2 = 1 \tag{27}$$

$$|S_{-a}|^2 + |S_{--}|^2 + |S_{-+}|^2 = 1 \tag{28}$$

$$|S_{+a}|^2 + |S_{-a}|^2 + |S_{aa}|^2 = 1. \tag{29}$$

These conditions express the conservation of flux in the three processes where the incoming excitation is a R^+ roton, a R^- roton and an atom, respectively. They reflect the fact that the present approach does not include inelastic channel. The unitarity of the S matrix gives three additional constraints:

$$S^*_{aa}S_{+a} + S^*_{a+}S_{++} + S^*_{a-}S_{+-} = 0 \tag{30}$$

$$S^*_{aa}S_{-a} + S^*_{a+}S_{-+} + S^*_{a-}S_{--} = 0 \tag{31}$$

$$S^*_{+a}S_{-a} + S^*_{++}S_{-+} + S^*_{+-}S_{--} = 0. \tag{32}$$

All these conditions for the scattering matrix elements can be used to obtain useful checks for the results of the numerical calculation.

5. RESULTS

The main results of the numerical analysis are shown in Fig. 5, where we report the probabilities $P_{ij} = |S_{ij}|^2$ as a function of energy. The data are obtained with several values of the parallel wave vector q_x in order to span the phonon forbidden region (region III of the spectrum in Fig. 1). The data at lowest energies in Fig. 5 correspond to $q_x = 0.6\ \text{Å}^{-1}$, the ones at highest energy to $q_x = 0.85\ \text{Å}^{-1}$. From the knowledge of the orthogonal wave vector q_z one extracts also the incidence angle. For R^+ and R^- rotons it is approximately $15° \div 20°$ and $20° \div 30°$, respectively, while for atoms is $50° \div 90°$. The range of incidence angles for rotons is rather

narrow, so that a discussion about the angular dependence of the evaporation and reflection probabilities is not significant in region III of the spectrum. Further work is planned to explore the angular dependence including region II. The error bars arise from fluctuations of the numerical results. They originate mainly from the fact that the states in the linear combination[19] may be not enough linearly independent. As explained at the end of Appendix C, this implies an amplification of small numerical uncertainties in the values of amplitudes, wave vectors and other parameters entering the expressions for P_{ij}.

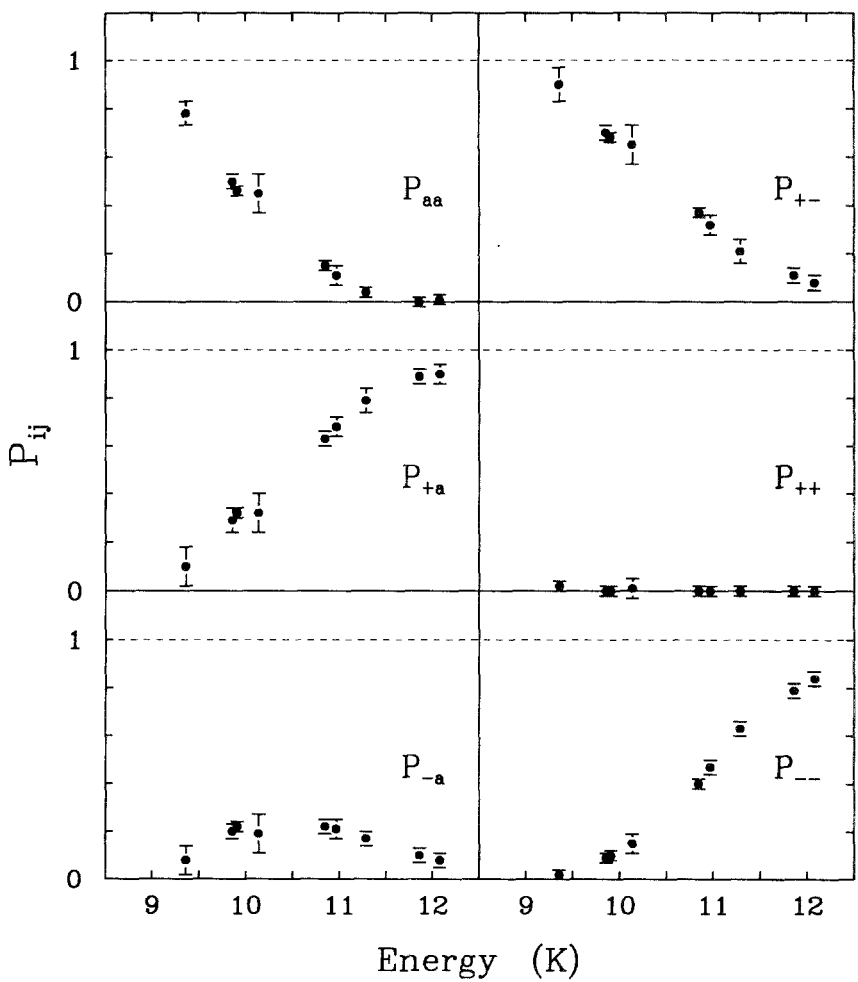

Fig. 5. Results for probabilities P_{ij} as a function of energy, in the phonon forbidden region.

Looking at Fig. 5 one notices that the unitarity conditions[27–29] are satisfied within the error bars. Actually each point with error bar corresponds to several combinations of states at the same energy. The unitarity condition can be checked for each combination separately. It turns out that it is satisfied within about 5% when the states in the combination are sufficiently linearly independent. An example of numerical values is given in Table I for states at energy 10.87 K. The results of different combinations of four states are given. The four states correspond to symmetric and antisymmetric solutions for two slabs (62 and 63.7 Å thick). One notes that the values of the probabilities P_{ij} extracted form different combinations are close each other. The unitarity conditions, which correspond to $\Sigma = 1$ in the notation of the table, is satisfied within 5% in all cases. Furthermore one has $P_{ij} \simeq P_{ji}$ as expected from Eq. (25).

The evaporation probabilities for R^+ and R^- rotons behave quite differently. The one for R^+ rotons grows from 0 to 1 by increasing the energy. A similar behavior has been recently observed in experiments at normal incidence in the same range of energy.[30] Conversely the R^- rotons are less effective in evaporating atoms. The ratio between the two probabilities has to be 1 at the energy Δ of the roton minimum where the two excitations become identical. As soon as the energy grows the ratio P_{+a}/P_{-a} increases and becomes large. Results for P_{+a}/P_{-a} are shown in Fig. 6.

At low energies, approaching Δ, the mode-change is dominant in the reflection processes for rotons. This is also consistent with symmetry arguments (see discussions in Ref. 21). At higher energies the mode-change becomes less probable. An incident R^- rotons has low probability of evaporating atoms, as discussed above, and it reflects as R^+ at low energy and as R^- at high energy. The behavior of an incident R^+ roton at high

TABLE I

Probabilities P_{ij} for Three Different Scattering Processes (Incident Atom, R^+ and R^-, Respectively) Described by Linear Combinations of Four States at the Same Energy, 10.87 K, and the Same Parallel Wave Vector, 0.7 Å^{-1}. The States 1-4 Are Symmetric (2 and 4) and Antisymmetric (1 and 3) Solutions for $L_{slab} = 62$ Å (1 and 2) and 63.7 Å (3 and 4), and for $L_{box} = 126$ Å (3), 134 Å (4) and 135 Å (1 and 2). The Quantity Σ Is the Sum of the Probabilities for Each Process

	atom → atom, R^+, R^-				R^+ → atom, R^+, R^-				R^- → atom, R^+, R^-			
Comb.	P_{aa}	P_{a+}	P_{a-}	Σ	P_{++}	P_{+-}	P_{+a}	Σ	P_{--}	P_{-+}	P_{-a}	Σ
1-2-3	0.148	0.654	0.224	1.026	0.0004	0.357	0.603	0.960	0.404	0.387	0.224	1.015
1-2-4	0.146	0.645	0.224	1.015	0.0003	0.358	0.612	0.970	0.403	0.385	0.228	1.016
1-3-4	0.148	0.650	0.223	1.021	0.0004	0.358	0.605	0.963	0.403	0.387	0.225	1.015
3-2-4	0.146	0.645	0.224	1.015	0.0004	0.358	0.612	0.970	0.404	0.384	0.228	1.016

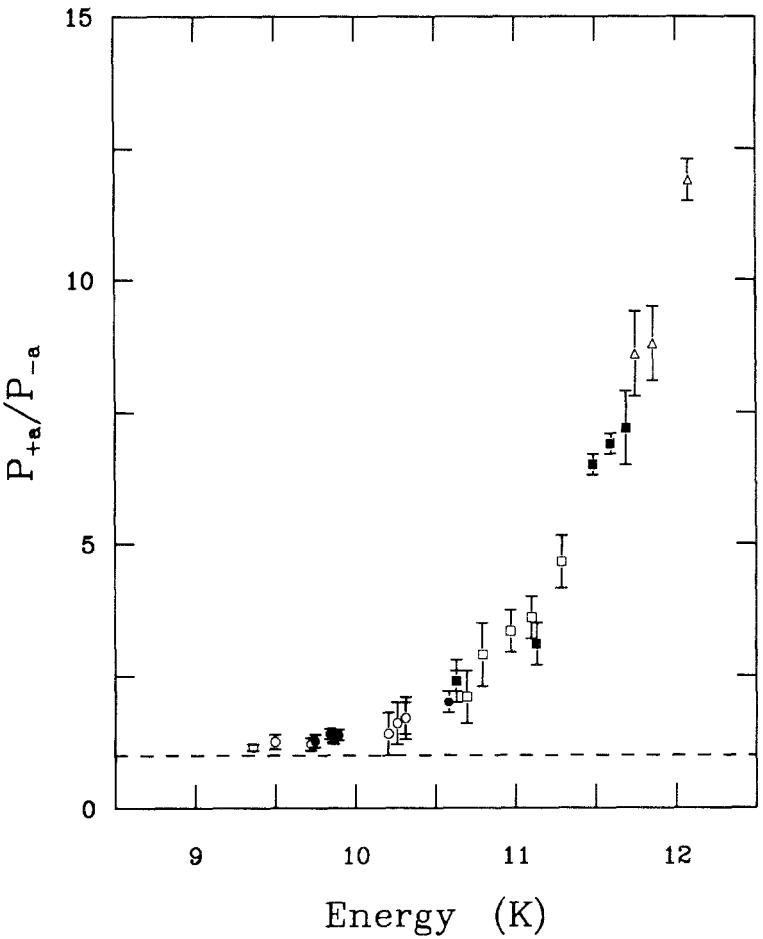

Fig. 6. Ratio of the evaporation probabilities for R^+ and R^- rotons as a function of energy. Open circles: $q_x = 0.6$ Å^{-1}; solid circles: $q_x = 0.65$ Å^{-1}; open squares: $q_x = 0.7$ Å^{-1}; solid squares: $q_x = 0.75$ Å^{-1}; triangles: $q_x = 0.8$ Å^{-1}. Dashed line: limiting value $P_{+a}/P_{-a} = 1$ for energy approaching $\Delta = 8.6$ K.

energy is completely different: the normal reflection as R^+ is found to be practically zero everywhere. R^+ rotons prefer to evaporate atoms or to reflect as R^-, the sum of the two probabilities being almost 1. This fact can be explained qualitatively by considering the change of momentum in a normal mode reflection. This should be twice $\hbar q_z$, where q_z in this part of the spectrum is of the order of 2 Å^{-1}. But it is difficult to imagine a mechanism for absorbing a momentum of the order of 4 Å^{-1} at the surface, the latter being quite smooth (the Fourier transform of the density profile

has vanishing components above 2 Å^{-1}). On the contrary, the momentum transfer for reflections involving R^- rotons is at least a factor two smaller and it is expected to be more probable.

The fact that P_{++} is almost zero everywhere has an interesting consequence. If we assume $S_{++}=0$ and use the unitarity conditions (27–32), we can express all the probabilities through a single parameter, for instance P_{+a}. Simple algebra gives (see Appendix D):

$$P_{+-}=1-P_{+a} \tag{33}$$

$$P_{--}=P_{+a}^2 \tag{34}$$

$$P_{aa}=P_{+-}^2=(1-P_{+a})^2 \tag{35}$$

$$P_{-a}=P_{-+}P_{+a}=(1-P_{+a})\,P_{+a}. \tag{36}$$

Note that the maximum value of P_{-a} from the last equation, is obtained for $P_{+a}=1/2$ and thus the following inequality holds:

$$P_{-a}\leqslant \tfrac{1}{4}. \tag{37}$$

All the above relations, which follow from the assumption $S_{++}=0$, are well satisfied by the numerical results in Fig. 5.

Finally, the results for the reflection probability for incident atoms are more intriguing. One knows from the experiments that the reflection probability is less than 1% apart from very small values of q_z where the long range Van der Waals interaction dominates. Our results for the reflection probability are consistent with the experimental results only at high energy, where P_{aa} drops to zero. At lower energy the roton channels become less and less active in the condensation process and the atom is reflected with large probability. This behavior is mainly the consequence of the fact that in the range of angles considered in the present work phonons cannot be excited. As soon as phonons are allowed (region I and II in Fig. 1) they are expected to provide the natural channel for the condensation of the incoming atoms. It has been also suggested that, as soon as the atom has enough energy to feel the external part of the density profile, it dissipates its energy by producing many low energy ripplons. This mechanism is not accounted for in our one-to-one theory.

6. CONCLUSIONS AND PERSPECTIVES

In this paper we have investigated the evaporation and condensation processes taking place at the free surface of superfluid helium. The main achievements of the present work concern both the formal development of

scattering theory, in the framework of linearised time dependent density functional formalism, and the numerical analysis, which provides first systematic results for the evaporation, condensation and reflection rates. The most relevant steps and achievements of our approach are here summarised:

- (i) The equations of motion of linearised time dependent density functional theory have been explicitly solved in the presence of the free surface using the Orsay-Trento phenomenological density functional. By taking linear combinations of different solutions carrying the same energy and momentum parallel to the surface, we have selected the relevant scattering processes (incoming atom reflected into an atom or condensed into a R^+ or R^- roton, etc.).
- (ii) We have identified, in the framework of the time dependent density functional scheme, the current of elementary excitations which obeys the equation of continuity (17) and allows one to evaluate the rates of evaporation and reflection. This current is determined by the group velocity and by the density of elementary excitations for which the familiar RPA expression (15) holds. The resulting formalism has been shown to be consistent with the general properties of the scattering matrix, following from unitarity and time reversal invariance.
- (iii) The numerical results, restricted in the present work to the region where only condensation of atoms into rotons is possible (region III of Fig. 1), reveal that rotons R^+ are systematically more effective than rotons R^- in the evaporation mechanism. An interesting feature emerging from our analysis, is that the P_{++} scattering probability is extremely small at all energies. This behavior, with the help of the formal properties of the scattering matrix, allows one to express all the evaporation and reflection rates in terms of a single parameter [see Eqs. (33–36)].
- (iv) A major discrepancy between our predictions and the experimental data concerns the atomic reflectivity which is predicted to be significantly large when the energy approaches the roton minimum. This behavior is easily understood since our theory accounts only for one-to-one processes where condensation into ripplons is excluded by the conservation laws. Due to the absence of phonon excitations, which are excluded in region III, no active excitations are allowed in the condensation process when the energy approaches the roton minimum with the consequent full reflection of the incident atom.

Natural developments of the present work will include:

- The study of the scattering process in different ranges of energy and incident angles, where phonons can participate in the scattering process.
- The study of multi-ripplon excitations whose effects can be taken into account through the use of an optical-type potential in the time dependent equations.

Work in these directions is in progress.

APPENDIX A. ORSAY-TRENTO DENSITY FUNCTIONAL

We use the phenomenological density functional of Ref. 20. It has the form:

$$E = E^{(kin)}[\rho, \mathbf{v}] + E^{(c)}[\rho] + E^{(bf)}[\rho, \mathbf{v}], \tag{A1}$$

where ρ and $\mathbf{v}$ are the density and velocity of the atoms, respectively. The first term is the kinetic energy of the non interacting bosons,

$$\begin{aligned} E^{(kin)}[\rho, \mathbf{v}] &= \int d\mathbf{r}\, \frac{\hbar^2}{2m} |\nabla \Psi(\mathbf{r})|^2 \\ &= \int d\mathbf{r} \left\{ \frac{\hbar^2}{2m} (\nabla \sqrt{\rho})^2 + \frac{m}{2} \rho(\mathbf{r})\, |\mathbf{v}(\mathbf{r})|^2 \right\}; \end{aligned} \tag{A2}$$

the correlation energy $E^{(c)}$ is given by

$$\begin{aligned} E^{(c)}[\rho] = \int d\mathbf{r} \Bigg\{ &\frac{1}{2} \int d\mathbf{r}'\, \rho(\mathbf{r})\, V_l(|\mathbf{r}-\mathbf{r}'|)\, \rho(\mathbf{r}') + \frac{c_2}{2} \rho(\mathbf{r})(\bar{\rho}_r)^2 + \frac{c_3}{3} \rho(\mathbf{r})(\bar{\rho}_r)^3 \\ &- \frac{\hbar^2}{4m} \alpha_s \int d\mathbf{r}'\, F(|\mathbf{r}-\mathbf{r}'|) \left(1 - \frac{\rho(\mathbf{r})}{\rho_{0s}}\right) \nabla\rho(\mathbf{r}) \cdot \nabla\rho(\mathbf{r}') \left(1 - \frac{\rho(\mathbf{r}')}{\rho_{0s}}\right) \Bigg\}; \end{aligned} \tag{A3}$$

finally, the backflow energy $E^{(bf)}$ is

$$E^{(bf)}[\rho, \mathbf{v}] = -\frac{m}{4} \iint d\mathbf{r}\, d\mathbf{r}'\, V_f(|\mathbf{r}-\mathbf{r}'|)\, \rho(\mathbf{r})\, \rho(\mathbf{r}')[\mathbf{v}(\mathbf{r}) - \mathbf{v}(\mathbf{r}')]^2. \tag{A4}$$

The first term in the kinetic energy, which depends on gradient of the density, is a quantum pressure; it corresponds to the zero temperature kinetic energy of non-interacting bosons of mass m. The two-body interaction V_l in the correlation energy $E^{(c)}$ is the Lennard–Jones interatomic potential,

TABLE II

Values of the Parameters Used in $V_J(\mathbf{r})$. See Eq. (A4)

γ_{11}	γ_{21}	γ_{12}	γ_{22}	α_1	α_2
-19.7544	-0.2395	$12.5616\ \text{Å}^{-2}$	$0.0312\ \text{Å}^{-2}$	$1.023\ \text{Å}^{-2}$	$0.14912\ \text{Å}^{-2}$

with the standard parameters $\alpha = 2.556$ Å and $\varepsilon = 10.22$ K, screened at short distance ($V \equiv 0$ for $r < h$, with $h = 2.1903$ Å). The two terms with the parameters $c_2 = -2.411857 \times 10^4$ K Å^6 and $c_3 = 1.858496 \times 10^6$ K Å^9 account phenomenologically for short range correlations between atoms. The weighted density $\bar{\rho}$ is the average of $\rho(\mathbf{r})$ over a sphere of radius h. Those terms are very similar to the functional of Ref. 24. The last term in $E^{(c)}$, depending on the gradient of the density in different points, has been added in order to improve the description of the static response function in the roton region. The function F is a simple Gaussian, $F(r) = \pi^{-3/2}\ell^{-3} \exp(-r^2/\ell^2)$ with $\ell = 1$ Å, while $\alpha_s = 54.31$ Å^3 and $\rho_{0_s} = 0.04$ Å^{-3}. The energy $E^{(bf)}$ contains an effective current-current interaction accounting for backflow-like correlations. In Ref. 20 the simple parametrisation

$$V_J(r) = (\gamma_{11} + \gamma_{12} r^2) \exp(-\alpha_1 r^2) + (\gamma_{21} + \gamma_{22} r^2) \exp(-\alpha_2 r^2) \qquad \text{(A5)}$$

was chosen in order to reproduce the phonon-roton dispersion in bulk liquid. The parameters are given in Table II.

APPENDIX B. EQUATION OF CONTINUITY AND CURRENT OF ELEMENTARY EXCITATIONS

In this appendix we show that definition (18) for the current of elementary excitations is consistent with equation (6) holding in time dependent density functional theory. In order to make the demonstration more transparent we use a simplified version of the energy functional of the form

$$\mathscr{H} = \frac{\hbar^2}{2m} |\nabla \Psi(\mathbf{r}_1)|^2 + \int d\mathbf{r}_2\, V(|\mathbf{r}_1 - \mathbf{r}_2|)\, \rho(\mathbf{r}_1)\, \rho(\mathbf{r}_2), \qquad \text{(B1)}$$

where V is a generic two-body interaction. The generalisation to the more complex Orsay–Trento functional is conceptually straightforward but rather tedious in practice.

Taking variations with respect Ψ^* in Eq. (6) one gets

$$\left[-i\hbar \frac{\partial}{\partial t} - \frac{\hbar^2}{2m} \nabla^2 + \int d\mathbf{r}_2\, V(|\mathbf{r}_1 - \mathbf{r}_2|)\, \rho(\mathbf{r}_2) - \mu \right] \Psi(\mathbf{r}_1, t) = 0. \qquad \text{(B2)}$$

Here we are interested in the solutions well inside the liquid, where the ground state density ρ_0 is a constant and the above equation yields

$$\mu = \rho_0 \int dr\ V(r). \tag{B3}$$

As in Eq. (9) we take a linear expansion of Ψ to describe the excited state. Let us include the time dependence in the definitions of f and g in the form

$$f(\mathbf{r}, t) = f e^{i(\mathbf{q}\cdot\mathbf{r} - \omega t)}; \qquad g(\mathbf{r}, t) = g e^{i(\mathbf{q}\cdot\mathbf{r} - \omega t)}, \tag{B4}$$

so that

$$\delta\Psi(\mathbf{r}, t) = f(\mathbf{r}, t) + g^*(\mathbf{r}, t). \tag{B5}$$

Inserting this expression in Eq. (B2) and isolating the terms oscillating with positive and negative frequencies, one gets two coupled equations for f and g:

$$-i\hbar \frac{\partial f(1)}{\partial t} - \frac{\hbar^2}{2m}\nabla^2 f(1) + \rho_0 \int d\mathbf{r}_2\, V(r_{12})[f(2) + g(2)] = 0 \tag{B6}$$

$$i\hbar \frac{\partial g(1)}{\partial t} - \frac{\hbar^2}{2m}\nabla^2 g(1) + \rho_0 \int d\mathbf{r}_2\, V(r_{12})[f(2) + g(2)] = 0 \tag{B7}$$

where we have used the short notation $(1) \equiv (\mathbf{r}_1, t)$ and $(2) \equiv (\mathbf{r}_2, t)$. Now, take $f(1)$ times the complex conjugate of Eq. (B6) and subtract $f^*(1)$ times Eq. (B6) itself. Similarly take $g(1)$ times the complex conjugate of Eq. (B7) and substract $g^*(1)$ times Eq. (B7). Summing up all the terms, one gets

$$\begin{aligned} i\hbar \frac{\partial}{\partial t}(|f(1)|^2 - |g(1)|^2) &= \frac{\hbar^2}{2m}[f(1)\nabla^2 f^*(1) - f^*(1)\nabla^2 f(1) + g(1)\nabla^2 g^*(1) - g^*(1)\nabla^2 g(1)] \\ &\quad - \rho_0 \int d\mathbf{r}_2\, V(r_{12})\{f(1) f^*(2) - f^*(1) f(2) + f(1) g^*(2) - g^*(1) f(2) \\ &\quad + g(1) f^*(2) - f^*(1) g(2) + g(1) g^*(2) - g^*(1) g(2)\}. \end{aligned} \tag{B8}$$

This equation has the form of an equation of continuity if the quantity

$$\rho^{ex} = |f(1)|^2 - |g(1)|^2 = f^2 - g^2 \tag{B9}$$

is interpreted as the density of elementary excitations and if the right hand side is identified with $-i\hbar\,\nabla\cdot\mathbf{j}^{ex}$. Now we prove that the quantity $\mathbf{j}^{ex}$ has indeed the form $\mathbf{j}^{ex}=\mathbf{v}\rho^{ex}$, where $\mathbf{v}$ is the group velocity of the excitation. To this purpose we rewrite properly the various terms in Eq. (B8). We begin with the one coming from the kinetic energy. All terms with the laplacian can be written in the form $-i\hbar\,\nabla\cdot[\mathbf{j}^{ex}]_{kin}$, with

$$[\mathbf{j}^{ex}]_{kin}=-\frac{\hbar}{2mi}[f(1)\,\nabla f^*(1)-f^*(1)\,\nabla f(1)+g(1)\,\nabla g^*(1)-g^*(1)\,\nabla g(1)]. \tag{B10}$$

We remember that $f(1)$ and $g(1)$ are plane waves, as in Eq. (B4). Thus the expression for $[\mathbf{j}^{ex}]_{kin}$, in terms of the real amplitudes f and g, becomes

$$[\mathbf{j}^{ex}]_{kin}=\frac{\hbar\mathbf{q}}{m}(f^2+g^2). \tag{B11}$$

To manage the terms containing the interaction is less trivial. Let us use the Fourier decomposition

$$f(\mathbf{r},t)=\int d\mathbf{q}_1\,f(\mathbf{q}_1,t)\,e^{i\mathbf{q}_1\cdot\mathbf{r}} \tag{B12}$$

and take the limit $f(\mathbf{q}_1)=f\,\delta(\mathbf{q}_1-\mathbf{q})$ at the end. We can rewrite the first two terms with the interaction in Eq. (B8) as

$$\int d\mathbf{r}_2\,V(r_{12})\{f(1)\,f^*(2)-f^*(1)\,f(2)\}$$

$$=\iint d\mathbf{q}_1\,d\mathbf{q}_2\,e^{i(\mathbf{q}_1-\mathbf{q}_2)\cdot\mathbf{r}_1}f(\mathbf{q}_1,t)\,f^*(\mathbf{q}_2,t)(V(\mathbf{q}_2)-V(\mathbf{q}_1)) \tag{B13}$$

where $V(\mathbf{q})$ is the Fourier transform of the interaction. By doing the same with the terms containing g, one gets

$$\begin{aligned}-i\hbar\,\nabla\cdot[\mathbf{j}^{ex}]_{pot}=-\rho_0\iint d\mathbf{q}_1\,d\mathbf{q}_2 e^{i(\mathbf{q}_1-\mathbf{q}_2)\cdot\mathbf{r}_1}(V(\mathbf{q}_2)-V(\mathbf{q}_1))\\ \times[f(\mathbf{q}_1,t)\,f^*(\mathbf{q}_2,t)+g(\mathbf{q}_1,t)\,g^*(\mathbf{q}_2,t)\\ +f(\mathbf{q}_1,t)\,g^*(\mathbf{q}_2,t)+g(\mathbf{q}_1,t)\,f^*(\mathbf{q}_2,t)].\end{aligned} \tag{B14}$$

Now, by considering $f(\mathbf{q})$ and $g(\mathbf{q})$ as delta functions, one gets

$$[\mathbf{j}^{ex}]_{pot}=\rho_0(f+g)(f^*+g^*)\,\nabla_q V(q) \tag{B15}$$

and summing $[\mathbf{j}^{ex}]_{pot}$ to $[\mathbf{j}^{ex}]_{kin}$ one finally obtains the result

$$\mathbf{j}^{ex} = \frac{\hbar \mathbf{q}}{m}(f^2 + g^2) + \rho_0(f+g)(f^* + g^*)\,\nabla_q V(q) \tag{B16}$$

for the total current. At this point it is convenient to rewrite Eq. (B16) in terms of the dispersion law $\omega(q)$ coming from the solutions of the equations of motion (B6–B7) which, for plane waves of the form (B4) and after some algebra, yield

$$f + g = \frac{\hbar q^2}{2m\omega}(f - g), \tag{B17}$$

$$f^2 + g^2 = \frac{2m}{\hbar q^2 \omega}\left[\omega^2 + \left(\frac{\hbar q^2}{2m}\right)^2\right](f^2 - g^2), \tag{B18}$$

with

$$\omega^2(q) = \frac{q^2}{2m}\left(\frac{\hbar^2 q^2}{2m} + 2\rho_0 V(q)\right). \tag{B19}$$

Inserting these results in Eq. (B16) one finally finds

$$\mathbf{j}^{ex} = \mathbf{v}(f^2 - g^2) = \mathbf{v}q^{ex}, \tag{B20}$$

where $\mathbf{v}$ coincides with the usual definition of the group velocity:

$$\mathbf{v} = \nabla_q \omega(q). \tag{B21}$$

This is the desired definition of the current density, in terms of which Eq. (B8) has the form of the equation of continuity (17):

$$\frac{\partial \rho^{ex}}{\partial t} + \nabla \cdot \mathbf{j}^{ex} = 0. \tag{B22}$$

APPENDIX C. DETERMINATION OF THE SCATTERING RATES

We give an example of derivation of the probabilities P_{ij} in the case of R^+ rotons coming to the surface and producing evaporated atoms and reflected R^+ and R^- rotons. The geometry we use is the one in Fig. 7: the surface is at $z = 0$, the center of the slab at $z = L$ and the left border of the box at $z = -b$. The solutions of our TDDF equations are real functions which vanish at $z = -b$. They can be either symmetric and antisymmetric with respect to the center of the slab ($z = L$). If b and L are sufficiently

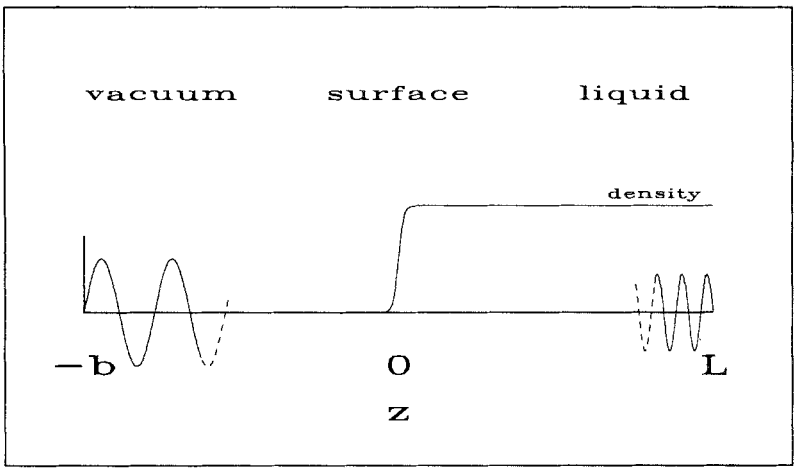

Fig. 7. Schematic picture for the geometry used in Appendix C.

large, the functions $f(z)$ and $g(z)$, characterising the changes $\delta\Psi$ as in Eq. (8), close to the boundary and near the origin are simple sinusoidal functions. In particular, close to $z=-b$ one has a free atom state of the form

$$f(z) \simeq f_a \sin[q_a(z+b)] = \frac{f_a}{2i} e^{iq_a b} e^{iq_a z} - \frac{f_a}{2i} e^{-iq_a b} e^{-iq_a z} \tag{C1}$$

and $g=0$. Close to $z=L$, inside the liquid, $f(z)$ is the sum of two oscillating functions of the form

$$f(z) \simeq f_{\pm} \sin[q_{\pm}(z-L)] = \frac{f_{\pm}}{2i} e^{-iq_{\pm} L} e^{iq_{\pm} z} - \frac{f_{\pm}}{2i} e^{iq_{\pm} L} e^{-iq_{\pm} z} \tag{C2}$$

in the antisymmetric case (a cosinus in the symmetric case) and the same for g. Here, for simplicity, the symbol q, for wave vectors, denotes the z-component only. The Fourier analysis of the solutions of the TDDF equations provides the amplitudes f_a and $f_{\pm}$ for fixed values of L and b. Changing L and b one can find different solutions at the same energy and parallel wave vector. Let us choose two symmetric states and an antisymmetric state and combine them in the form

$$f = f^{(1)}(z) + a_2 f^{(2)}(z) + a_3 f^{(3)}(z) \tag{C3}$$

where the solution $f^{(\alpha)}$ corresponds to the parameters L_α and b_α. The atomic part, well outside the slab, becomes

$$f_a = \frac{e^{iq_a z}}{2i}\left[f_a^{(1)} e^{iq_a b_1} + a_2 f_a^{(2)} e^{iq_a b_2} + a_3 f_a^{(3)} e^{iq_a b_3}\right] - \frac{e^{-iq_a z}}{2i}\left[f_a^{(1)} e^{-iq_a b_1} + a_2 f_a^{(2)} e^{-iq_a b_2} + a_3 f_a^{(3)} e^{-iq_a b_3}\right], \tag{C4}$$

the R^+ roton part, close to $z = L$, is

$$f_+ = \frac{e^{iq_+ z}}{2}\left[-i f_+^{(1)} e^{iq_+ b_1} + a_2 f_+^{(2)} e^{iq_+ b_2} + a_3 f_+^{(3)} e^{iq_+ b_3}\right] + \frac{e^{-iq_+ z}}{2}\left[i f_+^{(1)} e^{-iq_+ b_1} + a_2 f_+^{(2)} e^{-iq_+ b_2} + a_3 f_+^{(3)} e^{-iq_+ b_3}\right] \tag{C5}$$

and the R^- roton part is

$$f_- = \frac{e^{iq_- z}}{2}\left[-i f_-^{(1)} e^{iq_- b_1} + a_2 f_-^{(2)} e^{iq_- b_2} + a_3 f_-^{(3)} e^{iq_- b_3}\right] + \frac{e^{-iq_- z}}{2}\left[i f_-^{(1)} e^{-iq_- b_1} + a_2 f_-^{(2)} e^{-iq_- b_2} + a_3 f_-^{(3)} e^{-iq_- b_3}\right]. \tag{C6}$$

The quantities in brackets represent the amplitudes of incoming and outgoing excitations and one can choose the coefficients a_2 and a_3 in order to make two of them vanish. As said at the beginning, we show here the case of an incident roton R^+. So, we must have zero amplitude for incoming atoms and R^- rotons (see Fig. 4). Keeping in mind that R^- rotons travel with negative group velocity, one obtains the following algebraic equations for a_2 and a_3:

$$f_a^{(1)} e^{iq_a b_1} + a_2 f_a^{(2)} e^{iq_a b_2} + a_3 f_a^{(3)} e^{iq_a b_3} = 0 \tag{C7}$$

$$i f_-^{(1)} e^{-iq_- b_1} + a_2 f_-^{(2)} e^{-iq_- b_2} + a_3 f_-^{(3)} e^{-iq_- b_3} = 0. \tag{C8}$$

Since the ratio between the amplitude of the particle-hole f and the hole-particle g components depends only on the energy and not on the particular state in the combination, the above equations ensure that the incoming flux of atoms and R^- rotons vanish. One has to recall the definition (18) of the current density and use the values of a_2 and a_3 coming from Eqs. (C7–C8) in order to calculate the flux of the incoming rotons

and the ones of the outgoing excitations. The scattering rates come out to be:

$$P_{++} = \frac{|-iA_+^{(1)} e^{iq+b_1} + a_2 A_+^{(2)} e^{iq+b_2} + a_3 A_+^{(3)} e^{iq+b_3}|^2}{|iA_+^{(1)} e^{-iq+b_1} + a_2 A_+^{(2)} e^{-iq+b_2} + a_3 A_+^{(3)} e^{-iq+b_3}|^2} \tag{C9}$$

$$P_{+-} = \frac{|iA_+^{(1)} e^{-iq-b_1} + a_2 A_-^{(2)} e^{-iq-b_2} + a_3 A_-^{(3)} e^{-iq-b_3}|^2}{|iA_+^{(1)} e^{-iq+b_1} + a_2 A_+^{(2)} e^{-iq+b_2} + a_3 A_+^{(3)} e^{-iq+b_3}|^2} \tag{C10}$$

$$P_{+a} = \frac{|A_a^{(1)} e^{-iq_a b_1} + a_2 A_a^{(2)} e^{-iq_a b_2} + a_3 A_a^{(3)} e^{-iq_a b_3}|^2}{|iA_+^{(1)} e^{-iq+b_1} + a_2 A_+^{(2)} e^{-iq+b_2} + a_3 A_+^{(3)} e^{-iq+b_3}|^2} \tag{C11}$$

where $A_j = \text{sign}(f_j)\sqrt{v_j(f_j^2 - g_j^2)}$. One can also derive similar expressions using two anti-symmetric states and one symmetric state. The other scattering rates can be evaluated by selecting different processes, i.e., by solving different equations for the coefficients a_2 and a_3. The states entering the combinations have to be linearly independent. This requires a certain care in selecting proper values of L and b. If the states are not sufficiently independent, it happens that the denominators in the expressions for P_{ij} tend to be small and consequently small fluctuations in the numerical results produce large uncertainties in the final results.

APPENDIX D. UNITARITY CONDITION IN THE ABSENCE OF R^+ NORMAL REFLECTION

In this appendix we will derive expressions (33–36) for the scattering matrix elements in the phonon forbidden region (region III in the spectrum of Fig. 1) which are valid if $S_{++} = 0$. In this hypothesis one can rewrite Eqs. (27), (30) and (32), respectively, as

$$|S_{+a}|^2 + |S_{+-}|^2 = 1 \tag{D1}$$

$$S_{aa}^* S_{+a} + S_{a-}^* S_{+-} = 0 \tag{D2}$$

$$S_{+a}^* S_{-a} + S_{+-}^* S_{--} = 0. \tag{D3}$$

The first equation coincides with the result (33). From the other two one gets

$$S_{+-}^{*2} S_{--} = S_{+a}^{*2} S_{aa} \tag{D4}$$

or

$$|S_{+-}|^4 |S_{--}|^2 = |S_{+a}|^4 |S_{aa}|^2. \tag{D5}$$

Subtracting Eq. (29) from Eq. (28) one gets

$$|S_{+-}|^2 - |S_{+a}|^2 = |S_{aa}|^2 - |S_{--}|^2. \tag{D6}$$

Excluding S_{aa} from Eqs. (D5) and (D6) one finds

$$|S_{+-}|^2 + |S_{+a}|^2 = \left(\frac{|S_{-+}|^4}{|S_{+a}|^4} - 1 \right) |S_{--}|^2 \tag{D7}$$

or, using (D1):

$$|S_{--}|^2 = \left(\frac{|S_{+a}|^4 (|S_{+-}|^2 - |S_{+a}|^2)}{|S_{+-}|^4 - |S_{+a}|^4} \right) = \left(\frac{|S_{+a}|^4}{|S_{+-}|^2 + |S_{+a}|^2} \right) = |S_{+a}|^4. \tag{D8}$$

Thus we have obtained expression (34). Expression (35) can be derived in analogous way. Finally, by substituting (D1) and (D8) into (28), one finds

$$\begin{aligned} |S_{-a}|^2 &= 1 - |S_{+-}|^2 - |S_{--}|^2 \\ &= |S_{+a}|^2 - |S_{+a}|^4 \\ &= |S_{+a}|^2 |S_{-+}|^2 \end{aligned} \tag{D9}$$

which corresponds to the last result given in Eq. (36).

ACKNOWLEDGMENTS

We are indebted to A. F. G. Wyatt, A. C. Forbes, D. O. Edwards and M. Guilleumas for many useful discussions. L. P. thanks the hospitality of the Dipartimento di Fisica at the University of Trento as well as of the Institute for Condensed Matter Theory at the University of Karlsruhe and support of the Alexander von Humboldt Foundation.

REFERENCES

1. W. D. Johnston and J. G. King, *Phys. Rev. Lett.* **16**, 1191 (1966).
2. S. Balibar, J. Buechner, B. Castaing, C. Laroche, and A. Libchaber, *Phys. Rev. B* **18**, 3096 (1978).
3. D. O. Edwards, *Physica* **109** & **110B**, 1531 (1982), and references therein; V. V. Nayak, D. O. Edwards, and N. Masuhara, *Phys. Rev. Lett.* **50**, 990 (1983); S. Mukherjee, D. Candela, D. O. Edwards, and S. Kumar, *Jap. J. Appl. Phys.* **26-3**, 257 (1987).
4. M. J. Baird, F. R. Hope, and A. F. G. Wyatt, *Nature* **304**, 325 (1983); F. R. Hope, M. J. Baird, and A. F. G. Wyatt, *Phys. Rev. Lett.* **52**, 1528 (1984).
5. A. F. G. Wyatt, *Physica* **126B**, 392 (1984).
6. G. M. Wyborn and A. F. G. Wyatt, *Phys. Rev. Lett.* **65**, 345 (1990).
7. H. Baddar, D. O. Edwards, T. M. Levin, and M. S. Pettersen, *Physica B* **194-196**, 513 (1994).

8. C. Enss, S. R. Bandler, R. E. Lanou, H. J. Maris, T. More, F. S. Porter, and G. M. Seidel, *Physica B* **194-196**, 515 (1994)
9. A. F. G. Wyatt, M. A. H. Tucker, and R. F. Cregan, *Phys. Rev. Lett.* **74**, 5236 (1995).
10. A. C. Forbes and A. F. G. Wyatt, *J. Low Temp. Phys.* **101**, 537 (1995).
11. M. Brown and A. F. G. Wyatt, *J. Phys.: Condens. Matter* **2**, 5025 (1990).
12. A. Widom, *Phys. Lett.* **29A**, 96 (1969); D. S. Hyman, M. O. Scully, and A. Widom, *Phys. Rev.* **186**, 231 (1969).
13. P. W. Anderson, *Phys. Lett.* **29A**, 563 (1969).
14. M. W. Cole, *Phys. Rev. Lett.* **28**, 1622 (1972).
15. C. Caroli, B. Roulet, and D. Saint-James, *Phys. Rev. B* **13**, 3875, 3884 (1976).
16. D. P. Clogherty and W. Kohn, *Phys. Rev. B* **46**, 4921 (1992).
17. H. J. Maris, *J. Low Temp. Phys.* **87**, 773 (1992).
18. P. A. Mulheran and J. C. Inkson, *Phys. Rev. B* **46**, 5454 (1992).
19. F. Dalfovo, A. Fracchetti, A. Lastri, L. Pitaevskii, and S. Stringari, *Phys. Rev. Lett.* **75**, 2510 (1995).
20. F. Dalfovo, A. Lastri, L. Pricaupenko, S. Stringari, and J. Treiner, *Phys. Rev. B* **52**, 1193 (1995).
21. A. Lastri, F. Dalfovo, L. Pitaevskii, and S. Stringari, *J. Low Temp. Phys.* **98**, 227 (1995).
22. M. Casas, F. Dalfovo, A. Lastri, Ll. Serra, and S. Stringari, *Z. Phys. D* **35**, 67 (1995).
23. E. Krotscheck, in *Condensed Matter Theories*, M. Casas, M. de Llano, J. Navarro, and A. Polls eds. (Nova Science Pub., New York 1995) Vol. 10, p. 13.
24. J. Dupont-Roc, M. Himbert, N. Pavloff, and J. Treiner, *J. Low Temp. Phys.* **81**, 31 (1990).
25. L. B. Lurio *et al.*, *Phys. Rev. Lett.* **68**, 2628 (1992).
26. Note that in the same expansion written in Ref. 19 (Eq. (1)) there was a misprint in the sign of the argument of the exponential after $g(z)$.
27. The functions f and g in the notation of standard Bogoliubov theory are called u and v, respectively.
28. S. T. Beliaev, *Zh. Eksp. Teor. Fiz.* **34**, 417 (1958) [*Sov. Phys. JETP* **7**, 289 (1958)].
29. Different states at the same energy and wave vector can be found by varying the thickness of the slab and/or the size of the computational box. This procedure is equivalent to solve the equations of motion at fixed energy, slab and box, but different boundary conditions. We work with fixed boundary conditions (f and g vanish at the boundary).
30. A. C. Forbes and A. F. G. Wyatt, private communication.